NASA TECHNICAL NOTE

EARTH ORBITAL SATELLITE LIFETIME

by James E. Ladner and George C. Ragsdale

George C. Marshall Space Flight Center
Huntsville, Alabama

NATIONAL AERONAUTICS AND SPACE ADMINISTRATION • WASHINGTON, D. C. • JANUARY 1964

EARTH ORBITAL SATELLITE LIFETIME

By James E. Ladner and George C. Ragsdale

George C. Marshall Space Flight Center
Huntsville, Alabama

NATIONAL AERONAUTICS AND SPACE ADMINISTRATION

For sale by the Office of Technical Services, Department of Commerce,
Washington, D.C. 20230 -- Price $1.00

TABLE OF CONTENTS

LIST OF ILLUSTRATIONS

NATIONAL AERONAUTICS AND SPACE ADMINISTRATION

TECHNICAL NOTE D-1995

EARTH ORBITAL SATELLITE LIFETIME

By

James E. Ladner

and

George C. Ragsdale

SUMMARY

A definition of several factors important in the accurate prediction of orbital lifetime is presented. The factors are atmospheric variations, vehicle drag coefficient, propellant boiloff, and vehicle attitude stabilization. Curves are given for obtaining planning estimates of lifetime using a minimum number of vehicle and orbital parameters. Such estimates will have an uncertainty of +150 per cent and -70 per cent. The curves are valid for circular and eccentric orbits lying wholly between the altitudes of 150 and 500 km.

Solar radiation affects the atmosphere in two ways: a general expansion (or contraction) with the 11 year solar cycle and a diurnal bulge in the direction of the sun. Orbital lifetime may be increased by 150 per cent or decreased by 60 per cent due to the solar cycle effect. The diurnal bulge effect increases with altitude and may cause a decrease of 20 per cent for a 500-km circular orbit from the lifetime predicted by neglecting the bulge.

Recommended values for orbital drag coefficients of typical bodies are presented. These values are considered to have an uncertainty of ±25 per cent.

The loss of mass by a satellite (e.g., through propellant boiloff) will shorten its lifetime. Curves are presented for predicting the lifetime loss due to this effect.

The vehicle attitude stabilization affects the drag area presented for a particular vehicle. Two limiting cases of earth-fixed stabilization are limits encompassing all other types of stabilization including a tumbling vehicle.

I. INTRODUCTION

Plans for future space flights require accurate estimates of earth orbital lifetimes. In order to make an accurate lifetime estimate, a number of factors must be considered: atmospheric density, its variations due to seasonal, diurnal, and solar cycle effects, the vehicle drag coefficient, mass, and attitude stabilization. This report presents a definition of the magnitude of each of these factors, and attempts to estimate the uncertainty in lifetime predictions when they are both included and neglected.

II. METHOD FOR LIFETIME PREDICTION

The method used for calculation of lifetime estimates is essentially that developed by Sterne (Ref. 1). Several modifications to the method as previously applied (Ref. 2) have been added. These include improvement in the method of numerical integration, use of the 1959 ARDC model atmosphere, and inclusion of nonconstant values for vehicle drag coefficient, mass, and drag area.

Sterne's method is based on analytic expressions for the rate of change of apogee and perigee, which are integrated to yield orbital decay. The equations of Sterne as now modified are:

$$m(t)\ \frac{dp}{dt} = -\frac{A^{\frac{1}{2}}(1-e)K^{\frac{1}{2}}}{2\pi} \int_0^{2\pi} \rho A_o C_D \left[\frac{1+e\cos E}{1-e\cos E}\right]^{\frac{1}{2}} (1-\cos E)\, dE \quad (1)$$

$$m(t)\ \frac{da}{dt} = -\frac{A^{\frac{1}{2}}(1+e)K^{\frac{1}{2}}}{2\pi} \int_0^{2\pi} \rho A_o C_D \left[\frac{1+e\cos E}{1-e\cos E}\right]^{\frac{1}{2}} (1+\cos E)\, dE \quad (2)$$

$$\frac{dt}{da} = \frac{1}{\dot{a}} \quad (3)$$

$$\frac{dp}{da} = \frac{\dot{p}}{\dot{a}} \quad (4)$$

where the symbols are:

m = mass of satellite
t = time
p = perigee distance
a = apogee distance
A = orbit semi-major axis
e = orbit eccentricity
K = earth gravitation constant
ρ = atmospheric density
A_o = drag area
C_D = drag coefficient
E = Eccentric anomaly
$\dot{a} = \frac{da}{dt}$
$\dot{p} = \frac{dp}{dt}$

NASA TN D-1995

Equations (3) and (4) are integrated simultaneously by the Runge-Kutta method to yield the lifetime and perigee as a function of apogee. The integrals in (1) and (2) are evaluated by Simpson's rule. The terms A_o and C_D have been added under the integral sign. A_o and C_D may be functions of vehicle attitude, which in turn may be regarded as a function of E for most stabilization schemes. The atmospheric density is a function of the vehicle altitude and position relative to the diurnal bulge caused by the sun. The vehicle mass may be a function of time.

III. ATMOSPHERE

A. DESCRIPTION

Though much information about the upper atmosphere of the earth has been obtained in recent years from observation of earth satellites, a relatively high degree of uncertainty remains. It is known that the upper atmosphere is dynamic and is influenced primarily by radiation from the sun. The influence of this radiation increases with altitude, and is relatively small at altitudes below 100 km. The sun has two principal effects on the upper atmosphere.

First, radiation from the sun heats the atmosphere and causes it to expand, in addition to injecting particles into it. The expansion of the atmosphere produces a variation in density proportional to the degree of heating, which in turn depends upon the activity of the sun. Solar activity is commonly measured by the sunspot rate, which varies periodically over an 11 year cycle. The primary effect upon the atmosphere is a periodic variation in density over the 11 year cycle. Variations in solar activity, in addition to the 11 year cycle, produce less predictable variations in density.

Secondly, the heating of the atmosphere is greater on the side of the earth toward the sun, producing a bulge on that side. This bulge is located at approximately the same latitude as the sub-solar point, but lags the sun in time by 25 to 30 degrees longitude due to the rotation of the earth and its atmosphere. Thus, the peak in density for a given geographic location is reached at about 14 hours local time. The atmospheric bulge causes the density at a given point above the earth to vary diurnally, as the point rotates through the bulge every 24 hours, and seasonally, as the bulge moves with the sun in latitude from winter to summer.

The reference atmosphere most commonly used at the present time is the 1959 ARDC standard atmosphere (Ref. 3). However, this model atmosphere is inadequate to accurately predict satellite lifetimes, because it incorporates data averaged over a number of years for the entire surface of the earth. A recent survey and extrapolation of atmospheric data by Wasko is contained in Reference 4. This reference provides an extrapolation of atmospheric density for the current cycle of solar activity (July 1962 - July 1973), including the magnitude of the diurnal bulge.

B. EFFECT OF DIURNAL AND SEASONAL VARIATIONS OF ATMOSPHERIC DENSITY

1. Diurnal Model. Results of studies on the behavior of satellites in the upper atmosphere reveal that the diurnal fluctuations in density are of substantial magnitude and increase with increasing altitude, becoming the dominant feature of the atmospheric model above 300 km (Ref. 5).

The importance of the diurnal variations on the decay history of a satellite was shown by Jacchia for 1957 Beta One (Ref. 6). The "diurnal effect" was noted as a variation of acceleration with the geocentric angular distance between the sun and the satellite.

An empirical formula for atmospheric density was established by Jacchia (Ref. 7) to describe the observed phenomena of the solar effects within the limits of observational accuracy. Jacchia's formulation has been adapted to determine the atmospheric bulge relative to any known nighttime density profile and is presented as follows:

$$\rho = \rho o\,(Z) \left\{ 1+0.19 \left[e^{0.0055z} - 1.9 \right] \cos^{6} \psi/2 \right\} \qquad (5)$$

where

$\rho o\,(Z)$ Nighttime density profile
z Altitude (km)
ψ Angular distance between bulge and satellite.

At 180 degrees from the diurnal bulge (ψ = 180 degrees), the second term in the brackets will equal zero and density will be described by a nighttime density profile. (In these studies the 1959 ARDC model atmosphere was used as a reference, although it is not a nighttime profile.) For an altitude of 117 km, when $e^{0.0055z}$ equals 1.9, the second term also vanishes. Equation (5) was semi-empirically derived by Jacchia to explain observed satellite acceleration data. These data all pertained to altitudes above 117 km and the equation is not intended to represent lower altitudes. However, Jacchia indicates that there is little diurnal effect below some critical altitude (~ 117 km). Below this altitude solar radiation is absorbed and distributed uniformly throughout the bright and dark hemispheres. The equation is valid for altitudes between 117 and 700 km.

Using Jacchia's equation, the diurnal variation in density is seen in Figure 1 as a function of angular distance from the atmospheric bulge for altitudes of 200-600 km.

A comparison between the diurnal density variation as given by Jacchia's formula and as predicted by Wasko (Ref. 4) for three periods of solar activity is shown in Figure 2. The shapes of the two curves are in basic agreement for the altitude range of 200-600 km which is of primary importance here. Wasko's results, however, indicate a more dense diurnal bulge than that used in the study of the effect on lifetime, which would increase the magnitude of the effect somewhat beyond that shown in the following results.

2. Effect on Lifetime. This study has been limited by consideration of only circular orbits, use of Jacchia's model for the diurnal density variation, and assumption of a fixed geometry. The latter restriction means that the motion of the orbital plane through nodal regression and the motion of the sun are neglected. This is valid if the lifetimes considered are of sufficiently short duration. However, for accurate study of most lifetimes of practical interest (>1 week) nodal regression should be considered.

The results which will be shown are given as the change caused by the diurnal effect from the nominal lifetime which would be predicted using a diurnal mean atmosphere, i.e., an atmosphere valid at 0800 local time.

In order to illustrate the effect of variations in the position of the sun relative to the orbital plane, a 500-km orbit will be discussed. The effect of variations in parameters defining the sun-orbital plane relation is presented in Figures 3 and 4 for 500-km circular orbits. In these figures the per cent loss in lifetime from the lifetime predicted with a diurnal mean atmosphere is depicted as a function of orbit-sun geometry in order to illustrate the diurnal and seasonal effects on lifetime.

In Figure 3 for orbital inclinations of 0 and 40 degrees, lifetime curves are shown for sun declinations of 0, 10, and 20 degrees with variations in the difference between the right ascensions of the bulge center and the right ascension of the ascending node of the orbital plane (RA_B-RA_N). It can be seen that the curves are a straight line for an inclination of 0 degree (equatorial orbit) due to the fact that the sun is the same distance from the orbital plane for all right ascensions.

For an inclination of 0 degree and a declination of 0 degree the maximum lifetime loss is observed. In this case the earth-bulge center line is in the orbital plane. A minimum lifetime will be obtained whenever this particular geometry exists. For an inclination greater than the sun declination there are always two locations for the orbital node where this maximum lifetime loss occurs.

The minimum lifetime loss occurs when the angle between the bulge center and the orbital plane is greatest. This is realized for all positive solar declinations when the right ascension of the bulge is 270 degrees greater than that of the ascending node, and for negative solar declinations when the right ascension difference is 90 degrees. The minimum lifetime loss is further reduced as the difference between solar declination and orbital inclination is increased.

The effect of variations in orbital inclinations from 0 to 80 degrees is shown in Figure 4 for a sun declination of 20 degrees. In this figure, as in Figure 3, the maximum lifetime loss for a 500-km orbit is approximately 20 per cent of the nominal. For the minimum loss case (right ascension difference of 270 degrees for a +20 degrees solar declination), lifetime loss decreases as orbital inclination increases until an orbital inclination of 70 degrees is reached. Then the lifetime loss begins to increase. This reversal

occurs when the earth-bulge center line is perpendicular to the orbital plane (inclination 70, declination 20). The absolute minimum lifetime loss (i.e., the maximum lifetime) occurs whenever the earth-bulge center line is perpendicular to the orbital plane. In this geometry, a satellite encounters a diurnal mean atmosphere all along its orbital path.

3. Maximum Effect on Lifetime. From Figures 3 and 4 it is seen that the maximum lifetime loss (minimum lifetime) occurs when the earth-bulge center line lies in the orbital plane. The orbital path then passes directly through the atmospheric bulge and hence encounters an area of maximum drag. As long as the inclination of the orbit is equal to or greater than the sun's declination, this maximum drag condition will be realized for some value of the right ascension of the orbital node.

The extreme effect realized when the bulge center lies in the orbital plane may be used as the maximum possible loss of orbital lifetime from the diurnal effect when the orientation of the orbital plane relative to the sun is not known and cannot be restricted. If, however, the orientation can be restricted (e.g., the right ascension of the orbital plane ascending node is dependent on launch time), the accuracy of lifetime estimation can be increased.

Figure 5 presents the per cent of maximum lifetime loss as a function of altitude for circular orbits. As seen in the figure the maximum loss is almost a linear function of altitude, ranging from 4 per cent at 200 km to 20 per cent at 500 km.

It may be noted here that the regression of the orbital plane and the motion of the earth around the sun, which have been neglected in the numerical results shown, prevent the bulge center from remaining in the orbital plane for more than a short period of time. Hence, the maximum effect case given is realistically encountered only as a limit for short lifetimes.

C. EFFECT OF SOLAR ACTIVITY

Upper atmospheric density is influenced strongly by the activity of the sun. An increase in solar activity causes a corresponding increase in density. The activity of the sun goes through a complete cycle in approximately 11 years.

The predicted shift as derived by Wasko (Ref. 4) of mean diurnal atmospheric density from the 1959 ARDC model is presented in Figure 6 as a function of time. The curves are for altitudes in the 200 to 600-km region of the atmosphere. In general, the densities will be shifted more at higher altitudes than at lower ones. This is expected due to the fact that higher altitudes are more affected by solar activity.

The estimated effect of the extrapolated density shift on lifetimes predicted with the 1959 ARDC atmosphere is shown in Figure 7. In 1964 the decay rate of a given satellite should be approximately 112 per cent less than in 1969.

There is a substantial variation possible in the predicted mean density, that was illustrated in Figure 6, due to uncertainty in extrapolating solar activity and its effect on the atmosphere. Table I gives the estimated limits of density variation from the mean shown in Figure 6. The limits given are averaged for the 200 to 700-km altitude range from those given by Wasko as a function of altitude, and may be roughly interpreted as 2 σ variations.

TABLE I

UNCERTAINTY IN EXTRAPOLATED MEAN DIURNAL ATMOSPHERIC DENSITY

Possible Variation in Density	Per Cent Density Variations		
	Minimum Solar Activity Period	Medium Solar Activity Period	Maximum Solar Activity Period
Estimated Maximum Density Increase	130	130	75
Estimated Maximum Density Decrease	65	60	60

The various solar activity phases of the present eleven-year solar cycle are defined in the following manner:

1. Minimum (July 1962 - July 1966)
2. Medium (July 1966 - July 1967; January 1971 - July 1973)
3. Maximum (July 1967 - January 1971)

Based on the preceding table, it is estimated that total orbital lifetimes may be decreased as much as 60 per cent or increased as much as 150 per cent due to density variations from the mean values predicted. These may be regarded as 2 σ limits.

IV. DRAG COEFFICIENT

The many influences which affect the drag of a body in free molecular flow can be divided into two major categories, i.e., atmospheric and local body. Atmospheric influences include such parameters as composition of atmosphere, molecular mean free path, density, angle of attack, etc, while local body influences include parameters such as body material, surface lattice structure, body shape, etc. Formulation of all these influencing parameters into analytical expressions defining the degree of momentum and

energy accommodation has not been accomplished to any degree of satisfaction. Instead, empirical relations have been defined which oversimplify the mechanism underlying both momentum and energy accommodation.

For the prediction of orbital decay of large, stabilized, space vehicles, the simple assumption that the drag coefficient is 2.0 will no longer suffice. This assumption has been utilized in the past for the prediction of orbital lifetimes assuming an effective tumbling body. Numerous authors (see Ref. 8 through 12) have evaluated the drag coefficient of convex body shapes, confining their analysis to the two limiting cases, namely, diffuse re-emission and specular (mirror-like) reflection. These evaluations, in general, have been based on kinetic theory which is quite adequate in the expression of the motion of molecules impinging on a surface. However, as already stated, a large degree of uncertainty lies in the determination of the amount of accommodation (both momentum and energy), which is associated with the impingement of these molecules on the body surface.

The preliminary results of a literature survey (Ref. 13) have been utilized to obtain the recommended values for the drag coefficient of four body configurations assuming circular orbit velocity (Fig. 8). These configurations are: a cone with the free stream flow parallel to the longitudinal axis, a cylinder with the flow perpendicular to the longitudinal axis, a flat plate with the free stream flow normal to the surface, and a sphere.

Values of the diffuse drag coefficients presented in Figure 8 were calculated under the assumptions that the impinging molecules on a surface follow the Maxwellian velocity distribution law for gases at rest, or for isentropic gas flows (if an observer is at the body surface). It was assumed that a thermal accommodation process was assumed effected in the time interval in which the molecules are trapped at the wall since the temperature of the impinging molecule stream (~800° C at approximately 150 km) is not equal to the body surface temperature (~-10° C). This means the temperature of the re-emitted molecule stream has been assumed equal to the surface temperature of the body. Thus, the diffusely re-emitted molecules (most probable type of reflection) have random motions represented by a velocity distribution function corresponding to the re-emitted molecule temperature.

Specification of the mechanism underlying the interaction of the impinging molecules and the body surface is an area of large uncertainty in the calculation of the drag coefficient in free molecule flow. Simple empirical expressions have been defined, however, to express the degree of both energy (Ref. 14) and momentum (Ref. 15) accommodation. The thermal accommodation is represented as

$$\alpha = \frac{E_i - E_r}{E_i - E_w}$$

where E_i is the energy of the impinging molecules, E_r is the energy of the re-emitted molecules and E_w is the energy that the re-emitted molecules would have obtained if they

had been re-emitted in Maxwellian equilibrium with the body surface. This coefficient has been shown experimentally to be near unity for an air molecule impinging on an engineering surface. When considering other gas molecules (both monatomic and diatomic) a large degree of uncertainty arises due to the lack of adequate experimental results. Values of thermal accommodation have been measured experimentally, however, as low as 0.1, which represents the case of little or no accommodation.

Two interaction coefficients,

$$\sigma = \frac{\tau_i - \tau_r}{\tau_i}$$

and

$$\sigma' = \frac{P_i - P_r}{P_i - P_w},$$

have been specified to express the momentum accommodation where τ_i is the tangential momentum flux incident to the surface, τ_r that for the re-emitted molecules, P_i is the normal momentum incident to the surface, P_r that re-emitted, and P_w is the flux which would have been re-emitted if all of the molecules had been re-emitted in Maxwellian equilibrium with the surface. Adequate experimental information is also not available to determine the values of the above interaction coefficients, adding two additional factors of uncertainty to the prediction of the drag coefficient.

In lieu of adequate information, certain assumptions were made pertaining to the momentum and energy accommodation to obtain an overall factor of uncertainty. Since for engineering surfaces the interaction between a molecule and a surface is more nearly diffuse than specular, the following variations were assumed for the momentum and energy accommodation:

$$\sigma' \sim 1.0$$

$$0.85 < \sigma < 1.0$$

$$0 < \alpha < 1.0$$

The band of uncertainty shown in Figure 8 is based on 85 per cent accommodation of the tangential momentum component and 100 per cent accommodation of the normal momentum component and the two limiting cases of energy accommodation. Therefore, until more experimental data becomes available either from actual satellite flights or from low density wind tunnels, the drag coefficient for near-earth satellites should be based on diffuse re-emission with an associated uncertainty factor of approximately 25 per cent. This fact is in basic agreement with Schamberg (Ref. 12) who suggested for all convex body shapes a value of 2.5 ± 0.5 for the drag coefficient.

V. EFFECT OF VEHICLE MASS LOSS

The mass of a satellite is generally considered constant during its orbital lifetime; however, in the case of vehicles fueled with cryogenic liquids a significant mass loss may occur due to propellant boiloff. The loss of mass increases the drag deceleration of the vehicle and shortens the lifetime.

Figure 9 depicts the loss in total nominal lifetime due to mass loss. Nominal lifetime in this case is that which would be predicted for a constant initial mass. The per cent of lifetime loss is a function of the total propellant mass loss (measured in per cent of the total initial mass) and the boiloff time required for the mass loss as compared to the nominal lifetime. When the boiloff time is small in comparison to the nominal lifetime, the effect on total lifetime is the same as having the reduced mass after total boiloff throughout the entire lifetime. As the boiloff time becomes large in proportion to the nominal lifetime, the lifetime loss asymptotically approaches zero.

In a practical case, the Saturn S-IVB stage may have a boiloff time of about two weeks, while it might be desired to keep it in a parking orbit for perhaps a day. Under these conditions, a lifetime loss due to boiloff of about five per cent would result, and the parking orbit altitude must be chosen to allow for this factor.

VI. ATTITUDE STABILIZATION

A. EFFECTIVE DRAG AREA

The decay history of an orbiting vehicle is directly affected by the attitude stabilization assumed for the body, since attitude is a factor in the determination of both drag coefficient and effective area. The drag coefficient has been discussed previously in paragraph IV. Effective drag area is defined as the vehicle area projected normal to the atmospheric flow. The vehicle configuration, size, and angle of attack to the flow determine the projected area. The attitude stabilization of the vehicle controls the body orientation relative to the earth-fixed velocity vector and therefore controls the effective drag area.

B. TYPES OF STABILIZATION

1. No Stabilization. For tumbling bodies with no attitude control, the effective drag area changes as the vehicle turns. For a tumble period that is short in comparison to the orbital period an average area may be used. This average area is approximately the total surface area divided by 4 (Ref. 16).

2. Earth-Fixed Stabilization. In an earth-fixed stabilization the vehicle will keep a fixed orientation with respect to the local vertical of the earth and with respect to the orbital plane. The angle of attack between the velocity vector and the vehicle longitudinal axis will be constant if the orbit is circular, hence the effective drag area is constant. Two limiting cases with respect to drag area occur with earth-fixed stabilization. These are the cases where either the maximum or minimum possible projected area for a given body is obtained. For the slender cylindrical type bodies topped by a cone which are often encountered as space vehicles, these two cases are realized for angles of attack α of 90 degrees (broadside) and 0 degree (nose-on). Since the drag coefficient (par. IV) of a cylinder broadside is greater than that of a cone nose-on, the broadside and nose-on cases also represent limiting cases with respect to total drag. The ratio of the estimated broadside to nose-on drag for the Saturn SIVB + SII stage is 5.3, a factor which is directly carried into the orbital decay rate and lifetimes.

The two limiting cases of earth-fixed stabilization are also extreme limits encompassing all other types of stabilization including a tumbling vehicle. The ratio of estimated tumbling to broadside drag for the Saturn SIVB + SII stage is approximately 0.93, so that for this vehicle tumbling is almost equivalent to a broadside stabilization.

3. Space-Fixed Stabilization. In a space-fixed stabilization, the longitudinal axis is maintained in one constant inertial direction. This direction may be in the orbit plane or at some angle β to the plane. If β = 90 degrees, the drag area is constant and is effectively the same as for a 90 degree angle of-attack earth-fixed stabilization (maximum drag for a slender cylindrical vehicle). For all cases except the limit of β = 90 degrees, the angle of attack, and hence in general the effective area, will vary as the vehicle moves around its orbit.

The minimum effective drag area (maximum lifetime) for slender cylindrical bodies with space-fixed stabilization is obtained if the vehicle is stabilized with β = 0. In this case the longitudinal axis of the vehicle always lies in the orbital plane. The minimum drag for the SIVB + SII with space-fixed stabilization is 3.0 times that with the minimum drag earth-fixed stabilization (α = 0 degree).

In general, the angle β between the longitudinal axis and the orbital plane will not remain constant, due to the regression of the orbital node. Hence, the precise effect of space-fixed stabilization on the orbital decay rate of a vehicle can only be obtained for specific cases. Only if the time period of interest is short or special cases are encountered can the geometry be considered fixed. The limiting cases described can, however, be used in the absence of detailed information.

VII. SPECIAL PERTURBATION EFFECTS OF ORBITAL DRAG ON CIRCULAR ORBITS

If the drag on a vehicle in an initially circular orbit is uniform, the orbit will tend to remain circular. However, if the drag is not uniform, there will be a region of largest average drag somewhere along the orbital path, and one portion of the orbit will decay faster than the rest. The vehicle orbit will then tend to become elliptical, with a perigee developing 180 degrees away from the maximum drag region. Nonuniform drag can be produced by the diurnal atmospheric bulge or by variation in the ballistic factor $\frac{C_D A}{M}$ due to changing angle of attack.

Because the atmospheric density along the orbital path is not constant due to the diurnal bulge, orbits which initially are circular will become elliptical. The maximum amount of eccentricity due to the diurnal effect, which develops as a function of initial circular altitude, is shown in the upper part of Figure 10. As the orbit decays in altitude, the magnitude of the bulge decreases (Fig. 1). The orbit then tends to return to the circular condition for the remainder of its decay history. When the earth-bulge center line is perpendicular to the orbital plane, the diurnal effect is constant throughout the orbit as the angle between the sun and satellite is always 90 degrees. In this case an initially circular orbit remains circular.

A nonspherical vehicle that has a space-fixed orientation is also subjected to nonuniform drag as it proceeds along its orbital path, independent of atmospheric variations. If initially placed in a circular orbit, the vehicle orbit will become eccentric. The upper portion of Figure 10 also shows the maximum eccentricity due to the space-fixed attitude stabilization effect for the SIVB + SII vehicle as a function of initial altitude of the circular orbit. This curve serves only as an example, since the magnitude of this effect is a function of the particular vehicle configuration under consideration. The tendency to become eccentric continues throughout the entire lifetime so that the maximum eccentricity is realized at the end of the lifetime. The approximate eccentricity rate for initially circular orbits as a function of the initial altitude is depicted in the lower portion of Figure 10 for an SIVB + SII vehicle.

VIII. NOMINAL LIFETIME PREDICTIONS

A. DESCRIPTION

In previous sections of this report we have defined some significant factors in the accurate estimation of satellite lifetimes. We now present nominal lifetime curves (Fig. 11 and 12) which may be used to obtain a planning estimate of lifetime. In using these results, a distinction must be made between the quantities of total and useful lifetime. The curves which will be presented are for total lifetime, i.e., total staytime

in orbit before re-entry. Prediction is usually desired, however, for the length of time that will be useful for a specified purpose, i.e., during which certain orbital conditions will be satisfied. The portion of the total lifetime that is useful is difficult to generalize, since it depends upon the specific orbital mission. It may often be significantly less than the total lifetime. The definition of useful lifetime has not been attempted in this report. However, the curves presented may be used not only to define total lifetime but also decay time between given orbital altitudes. The curves given are based on the 1959 ARDC model atmosphere. They do not contain the diurnal bulge and assume the vehicle weight, area, and drag coefficient to be constant. To use these curves it is necessary to know only the vehicle weight (sea level), drag area, approximate drag coefficient and altitude of the orbit desired. The uncertainty of a nominal estimate so obtained is +150 per cent and -70 per cent. Circular orbits ranging in altitude from 150 to 500 km are covered. Eccentric orbits are covered for apogee and perigee values both lying within this altitude range.

B. PROCEDURE FOR USE

The stepwise procedure required to use the curves is as follows:

1. Determine drag coefficient, C_D

Cone, nose-on	~2.2
Cylinder, broadside	~2.75

2. Determine the projected area in square meters, A.

	Nose-on ($\alpha = 0°$)	Broadside ($\alpha = 90°$)
Cone	$A = \frac{\pi D^2}{4}$	$A = \frac{DL}{2}$
Cylinder	$A = \frac{\pi D^2}{4}$	$A = DL$

A = Projected area (m^2)

D = Vehicle diameter (m)

L = Vehicle Length (m)

α = Angle of attack

3. Determine weight in kilograms, W

4. Compute the ratio $\frac{W}{C_D A}$ in kg/m^2

5. Read normalized lifetime value from curves for the apogee and perigee desired.

6. To obtain the total lifetime in days, multiply W/C_DA by the value read from the graph.

If something more than the minimum information is known about a particular case, then the following formula may be applied to adjust the nominal value of lifetime for the predicted atmospheric effects and propellant boiloff.

$$L_T = L_N (1 + \Delta so - \Delta D_i - \Delta Bo) \pm U \qquad (6)$$

L_T = Total lifetime estimate

L_N = Nominal value from curves times $\frac{W}{C_D A}$

Δso = Per cent change (plus or minus) from 1959 ARDC atmosphere as a function of year of launch (Fig. 7)

ΔDi = Per cent loss due to the diurnal bulge effect (Fig. 5 for limiting effect)

ΔBo = Per cent loss due to propellant boiloff (Fig. 9)

U = Uncertainty due to drag coefficient, and the prediction of the Solar activity, equal to +150 per cent or - 60 per cent.

Other than total lifetime, several other quantities can be obtained by using these nominal curves. Equation (6) may be used with the curves to obtain the altitude necessary to insure a certain lifetime. The total required orbital lifetime L_T must be known; this will in general be somewhat greater than the desired operational lifetime of the useful satellite. Equation (6) may then be solved for a corresponding value of L_N. The nominal curves are entered with this value of $L_N \cdot \frac{C_DA}{W}$ to obtain either a required circular altitude or an apogee and perigee combination which will produce the desired lifetime.

The time spent in decaying from one circular altitude to another can also be found by subtracting the respective lifetime values. For elliptical orbits, the time spent in decaying from one apogee to another could be found in a like manner if the perigee could be assumed fixed. However, for the altitude range presented here this assumption would cause an error of approximately 20 to 30 per cent, since the perigee in all cases experiences a decay whose effect cannot be neglected.

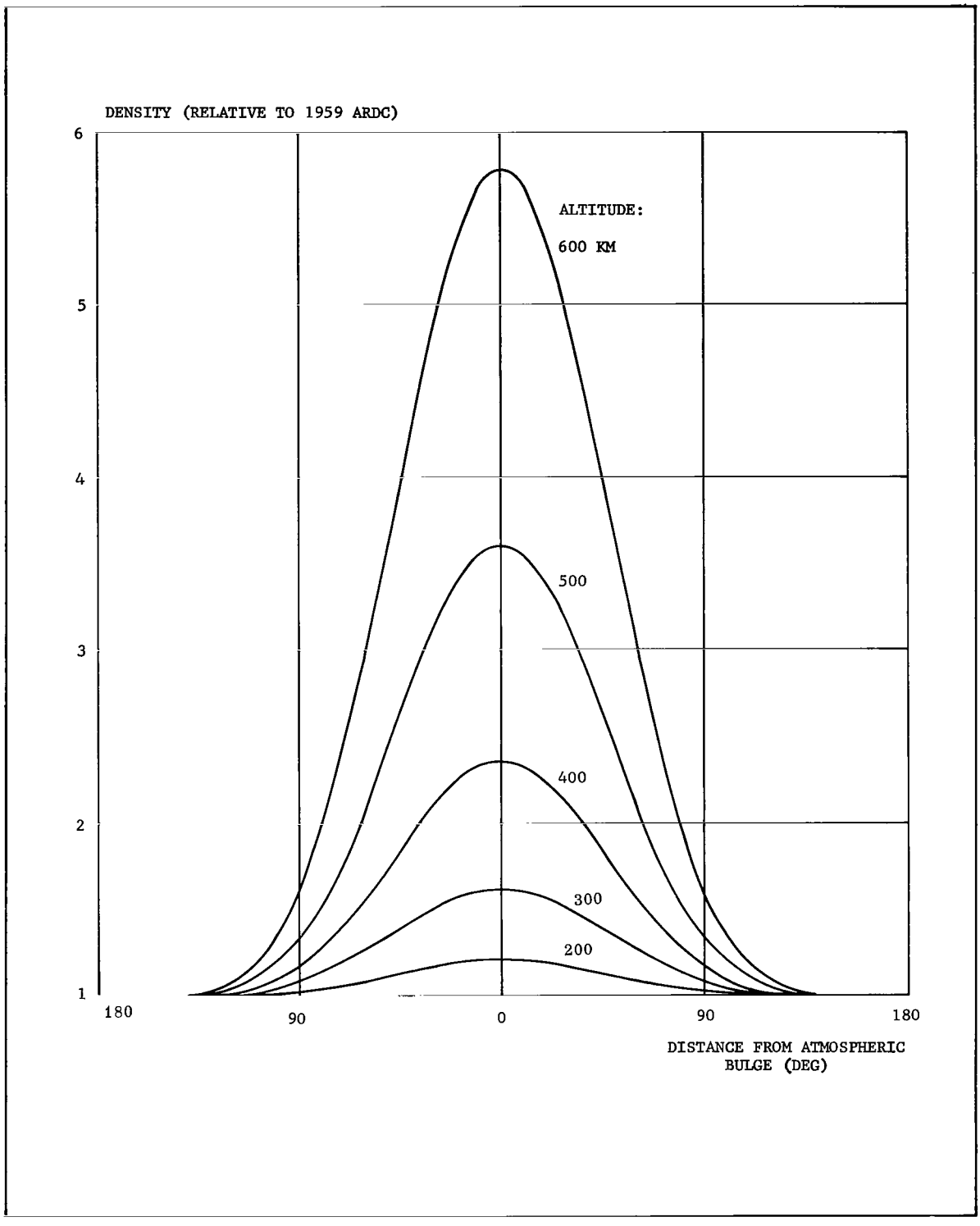

FIGURE 1. DIURNAL VARIATIONS IN ATMOSPHERIC DENSITY

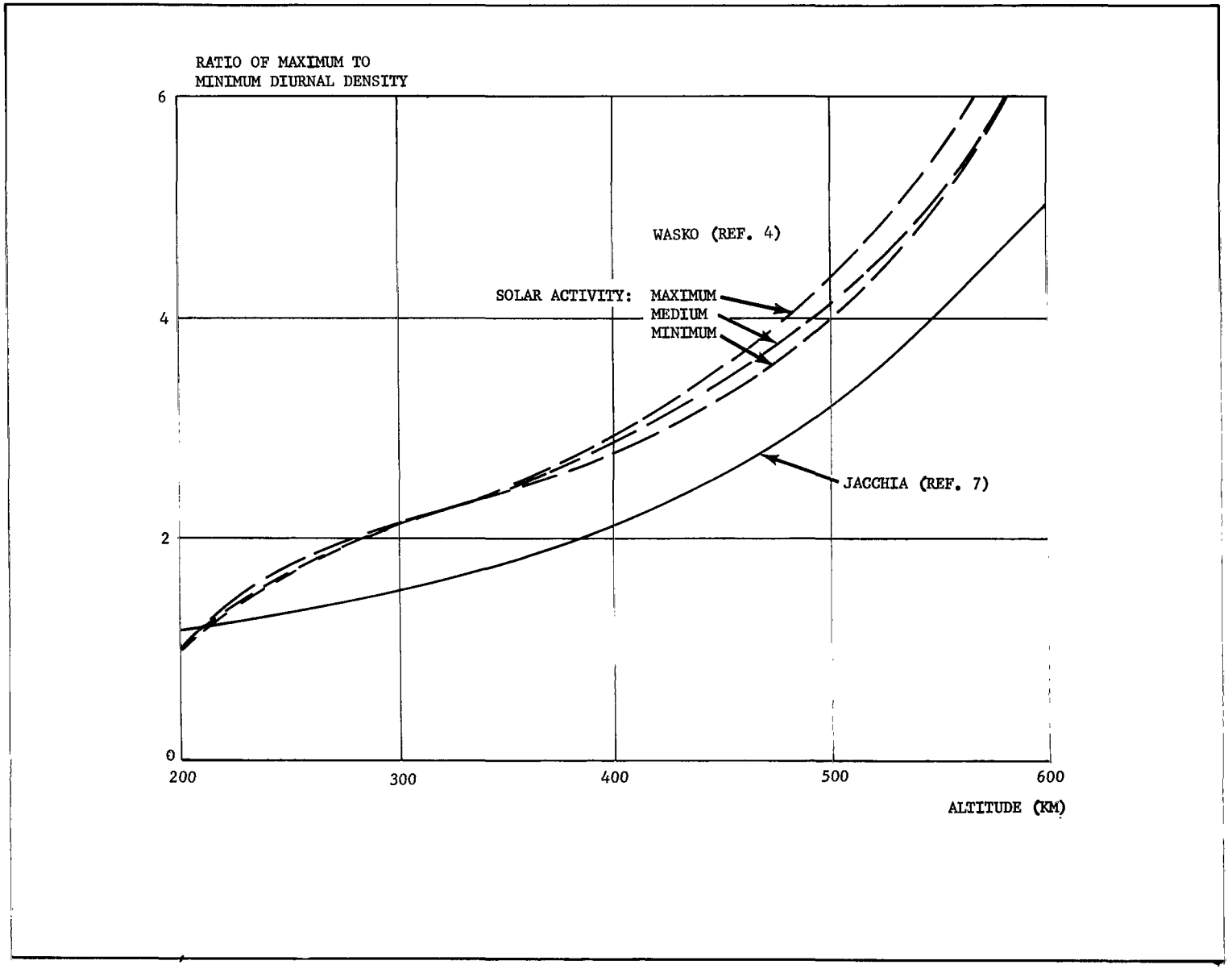

FIGURE 2. COMPARISON OF MAXIMUM DIURNAL DENSITIES

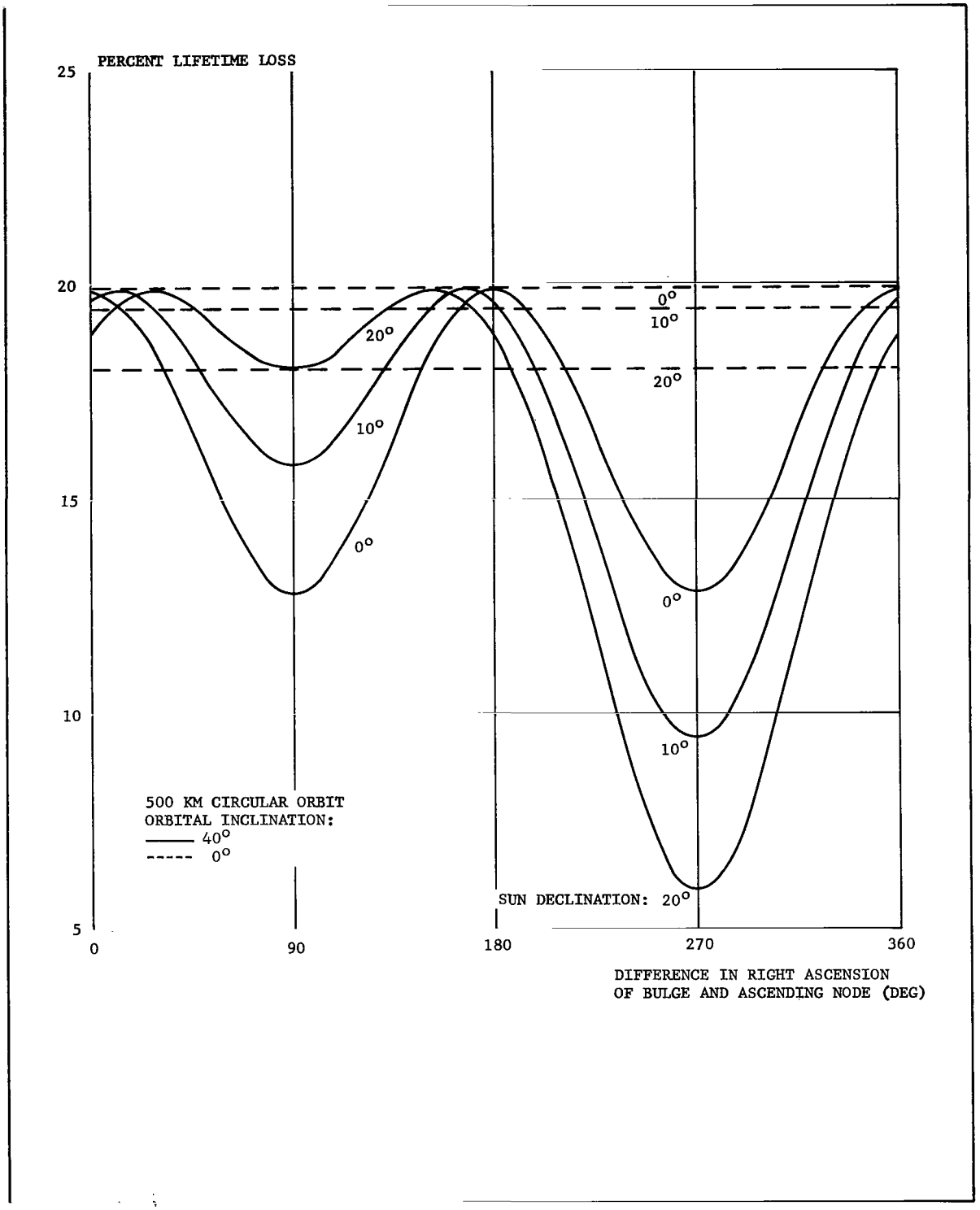

FIGURE 3. LIFETIME LOSS FROM DIURNAL BULGE: EFFECT OF SOLAR POSITION

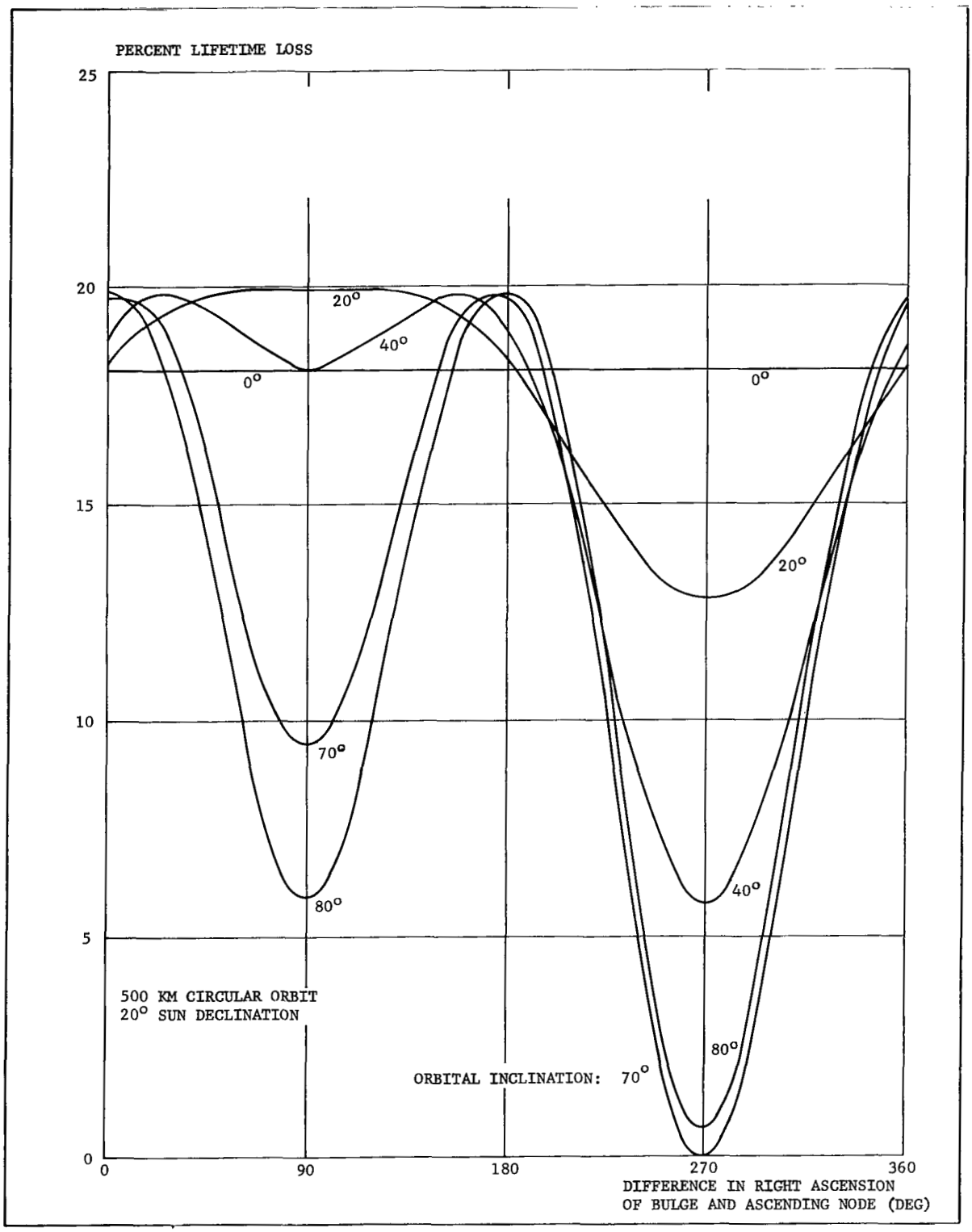

FIGURE 4. LIFETIME LOSS FROM DIURNAL BULGE: EFFECT OF ORBITAL POSITION

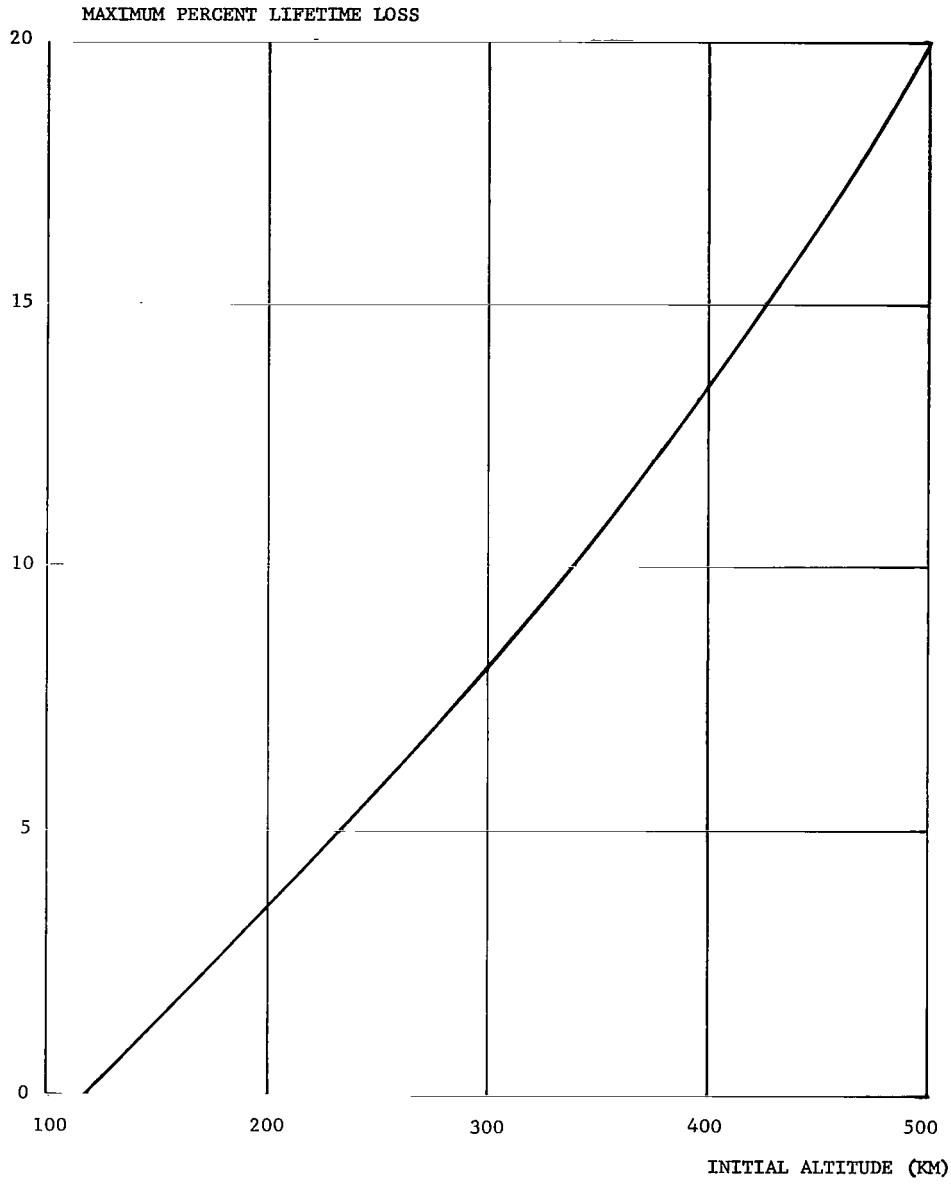

FIGURE 5. LIFETIME LOSS FROM DIURNAL BULGE: MAXIMUM EFFECT

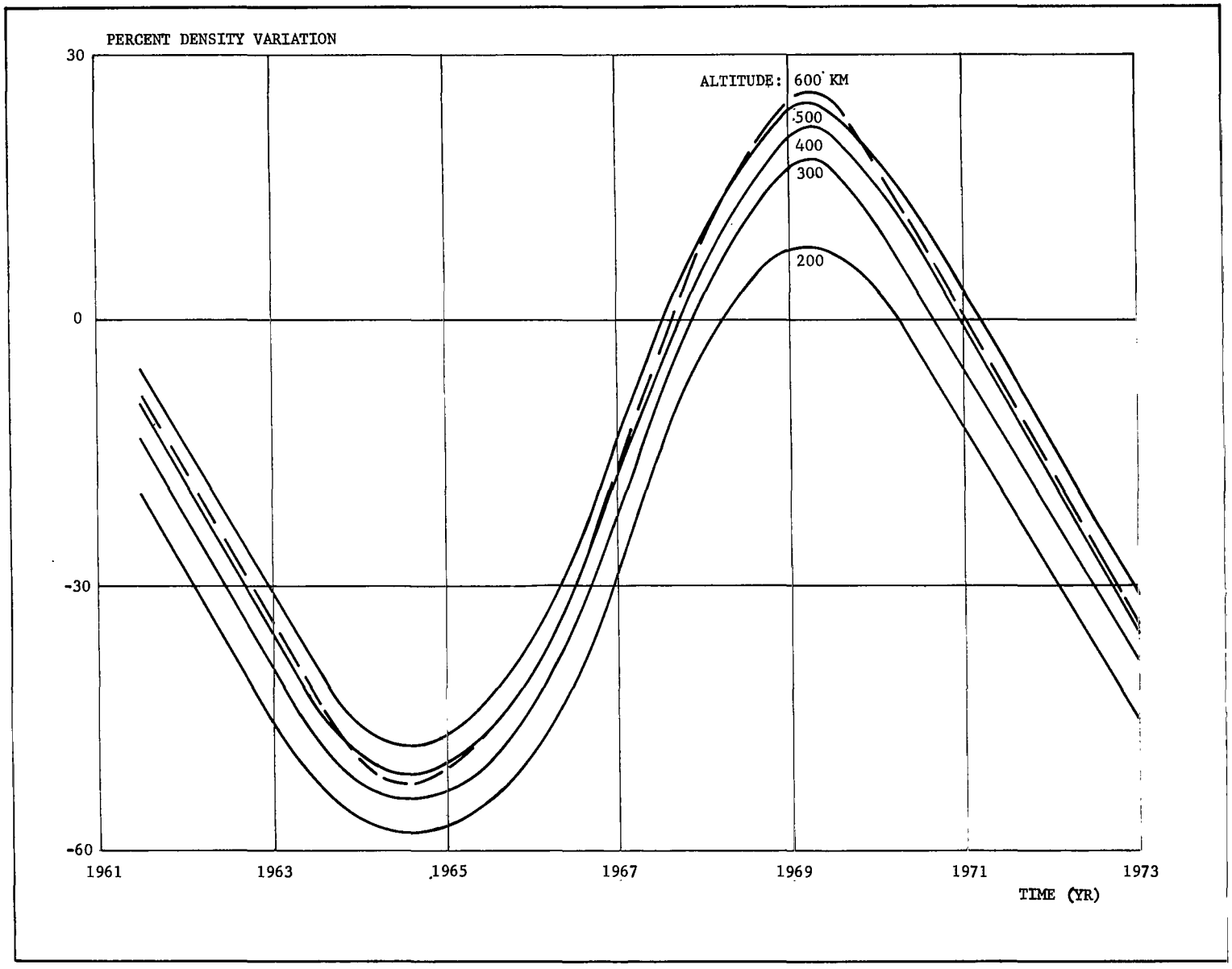

FIGURE 6. PREDICTED DENSITY VARIATION FROM 1959 ARDC ATMOSPHERE

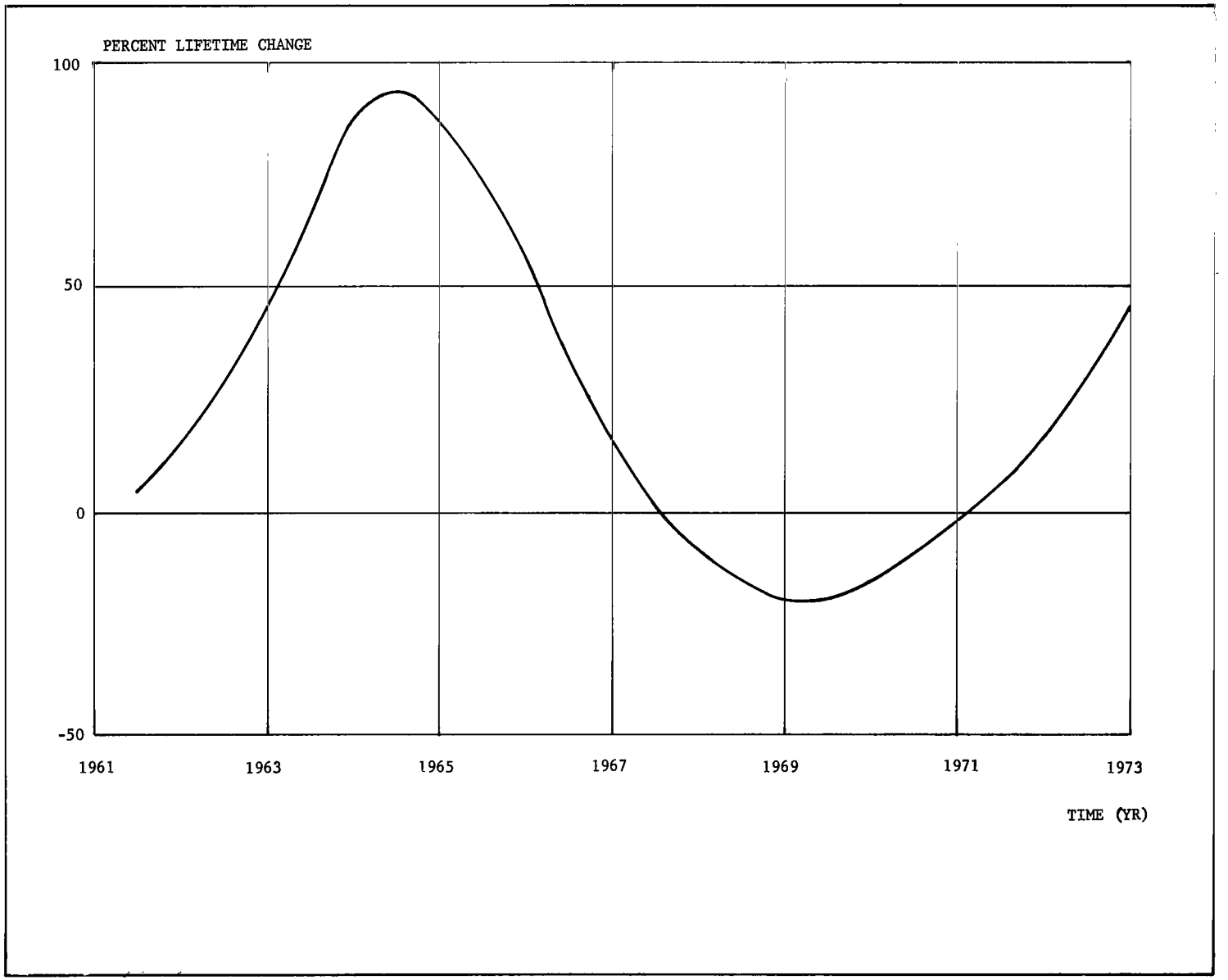

FIGURE 7. ESTIMATED LIFETIME CHANGE DUE TO PREDICTED DENSITY VARIATIONS

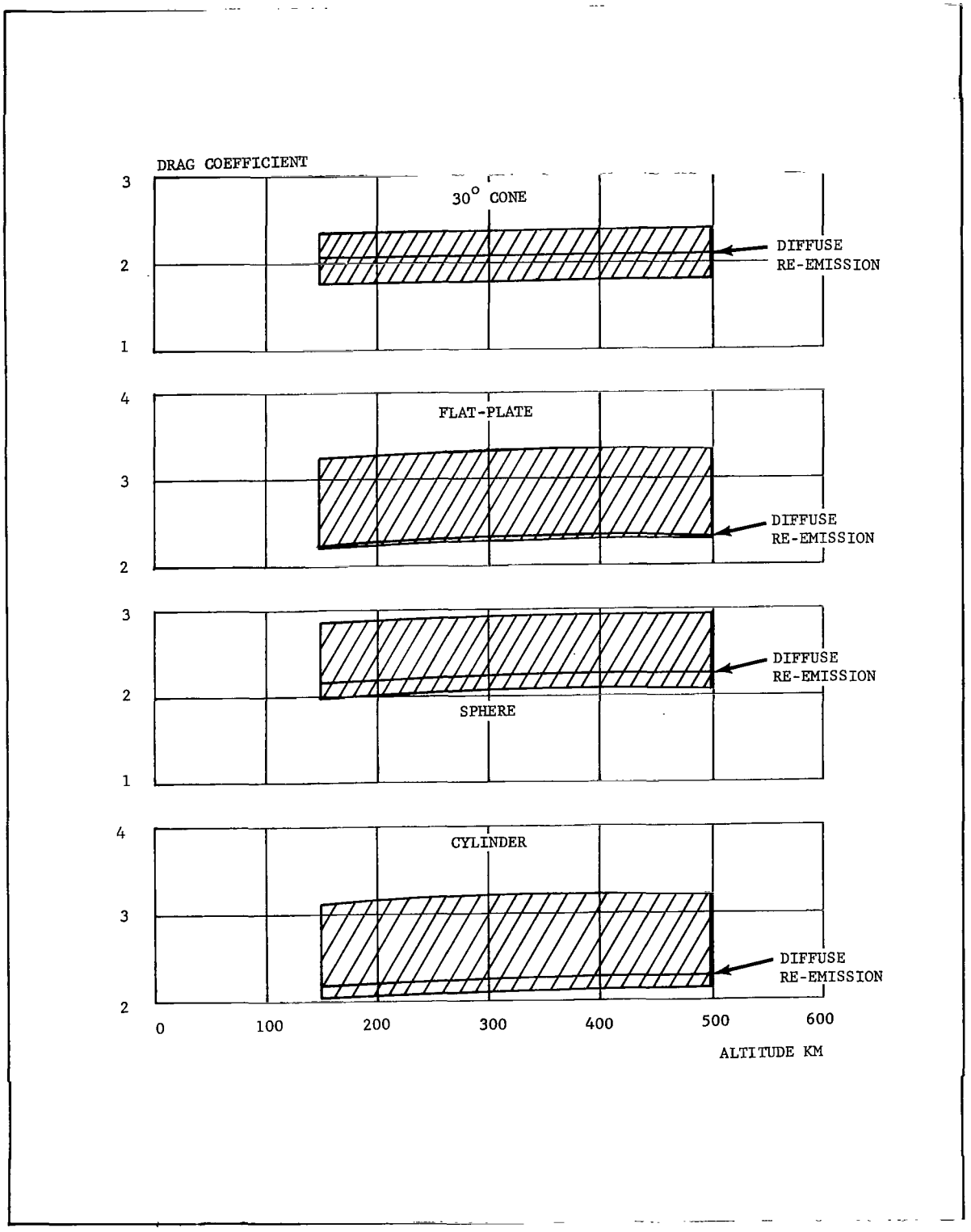

FIGURE 8. ESTIMATED DRAG COEFFICIENTS

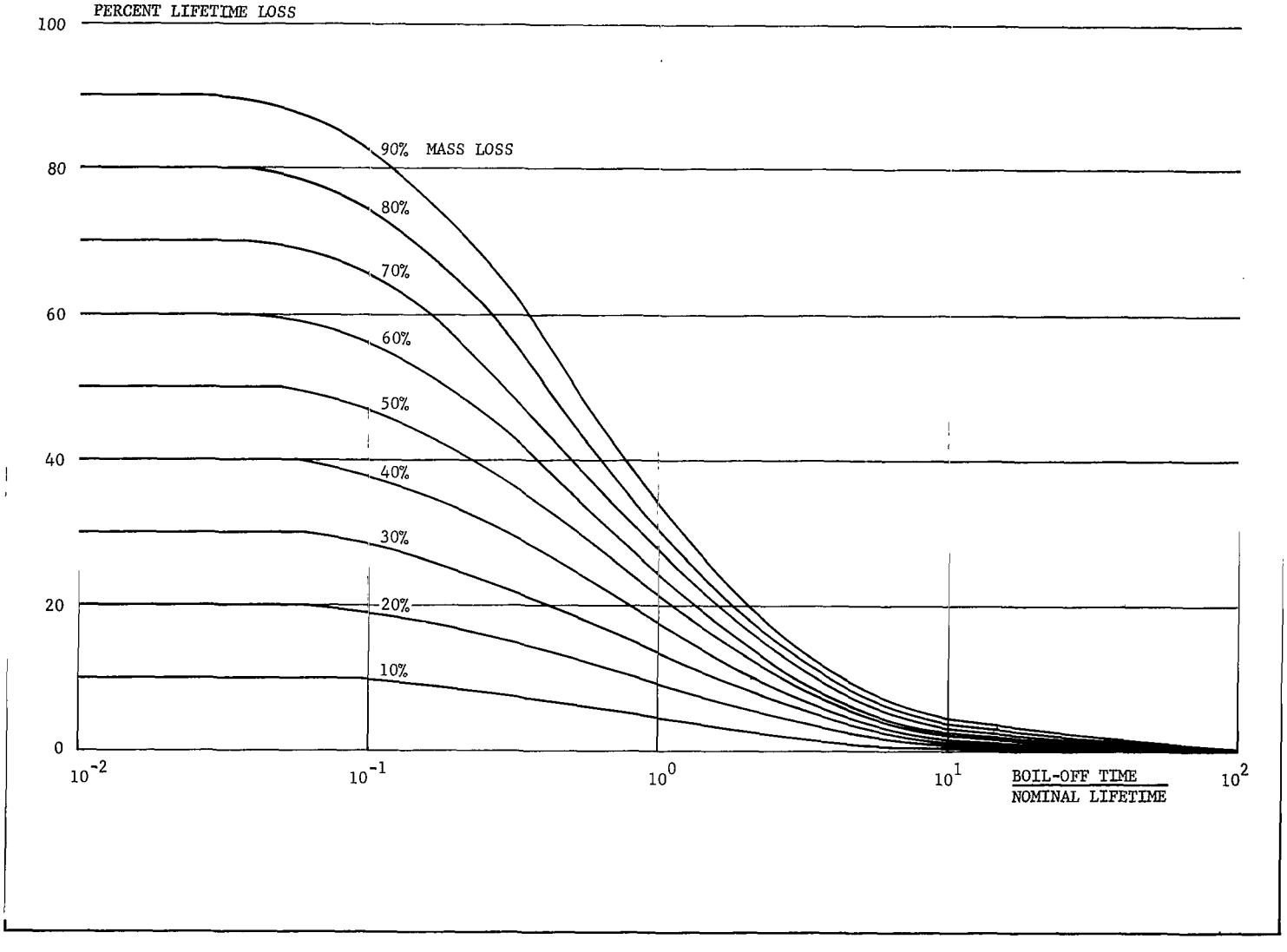

FIGURE 9. EFFECT OF MASS LOSS ON LIFETIME

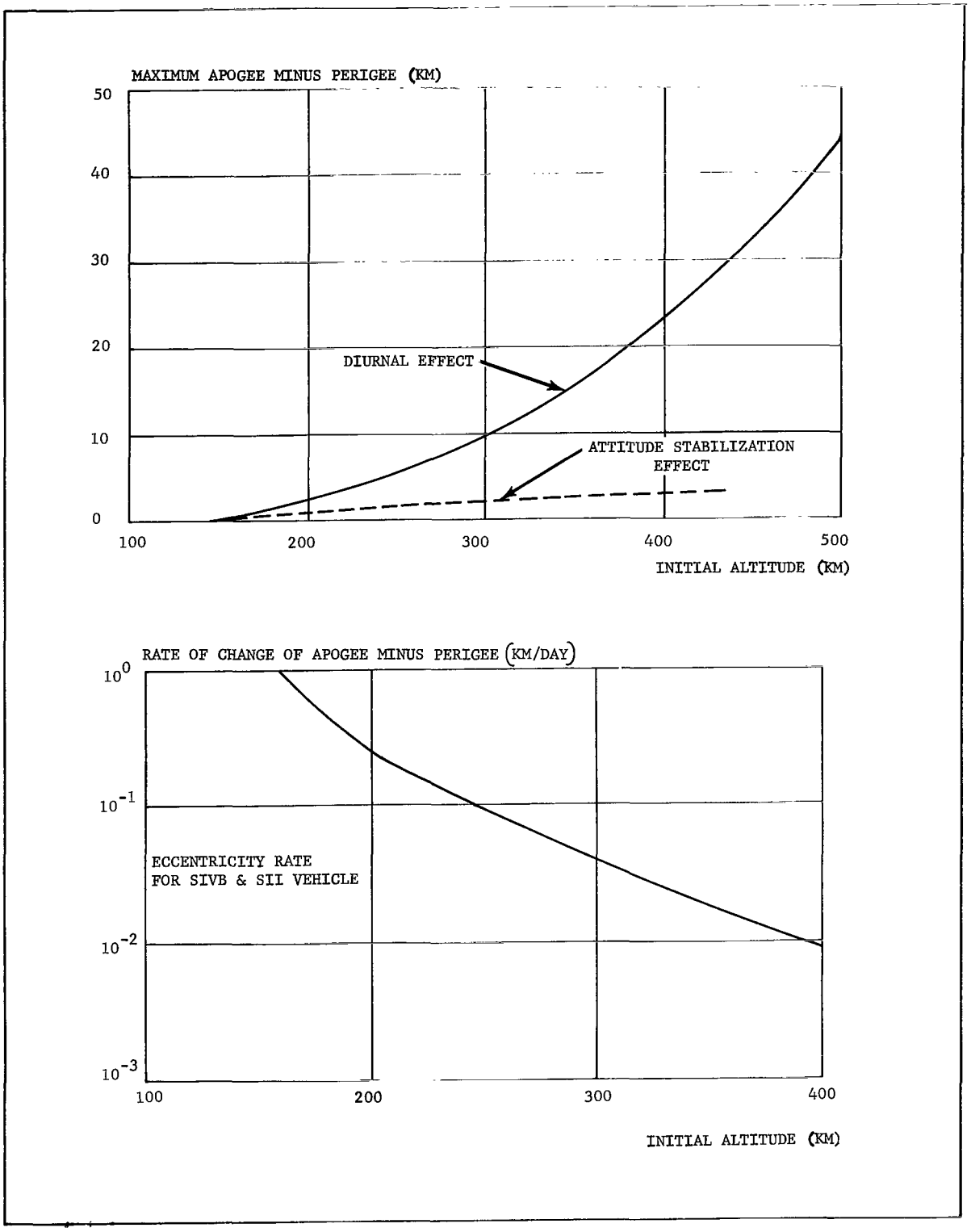

FIGURE 10. EFFECT OF DRAG ON ORBITAL ECCENTRICITY

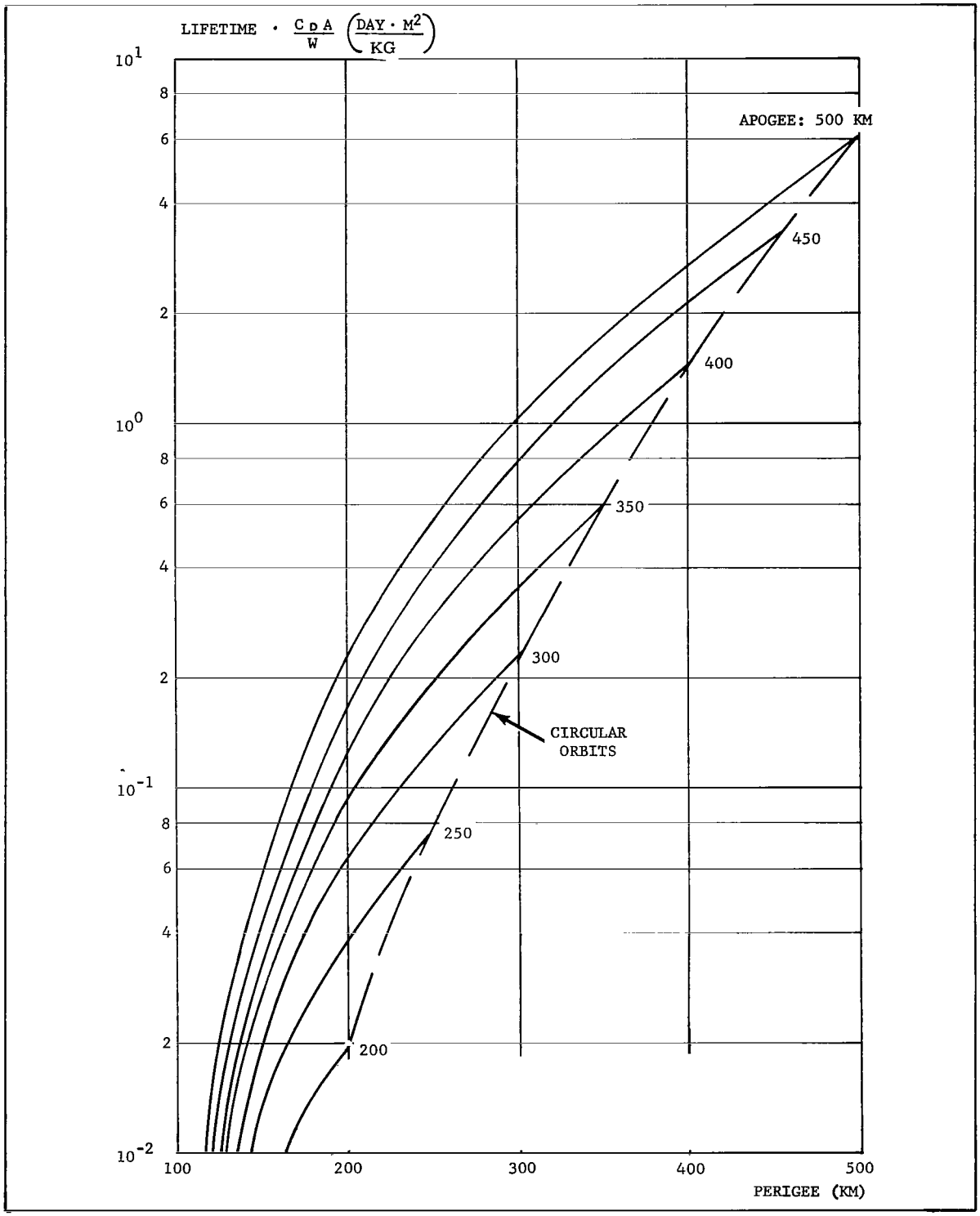

FIGURE 11. ORBITAL LIFETIME: 100-500 KM ALTITUDE REGION

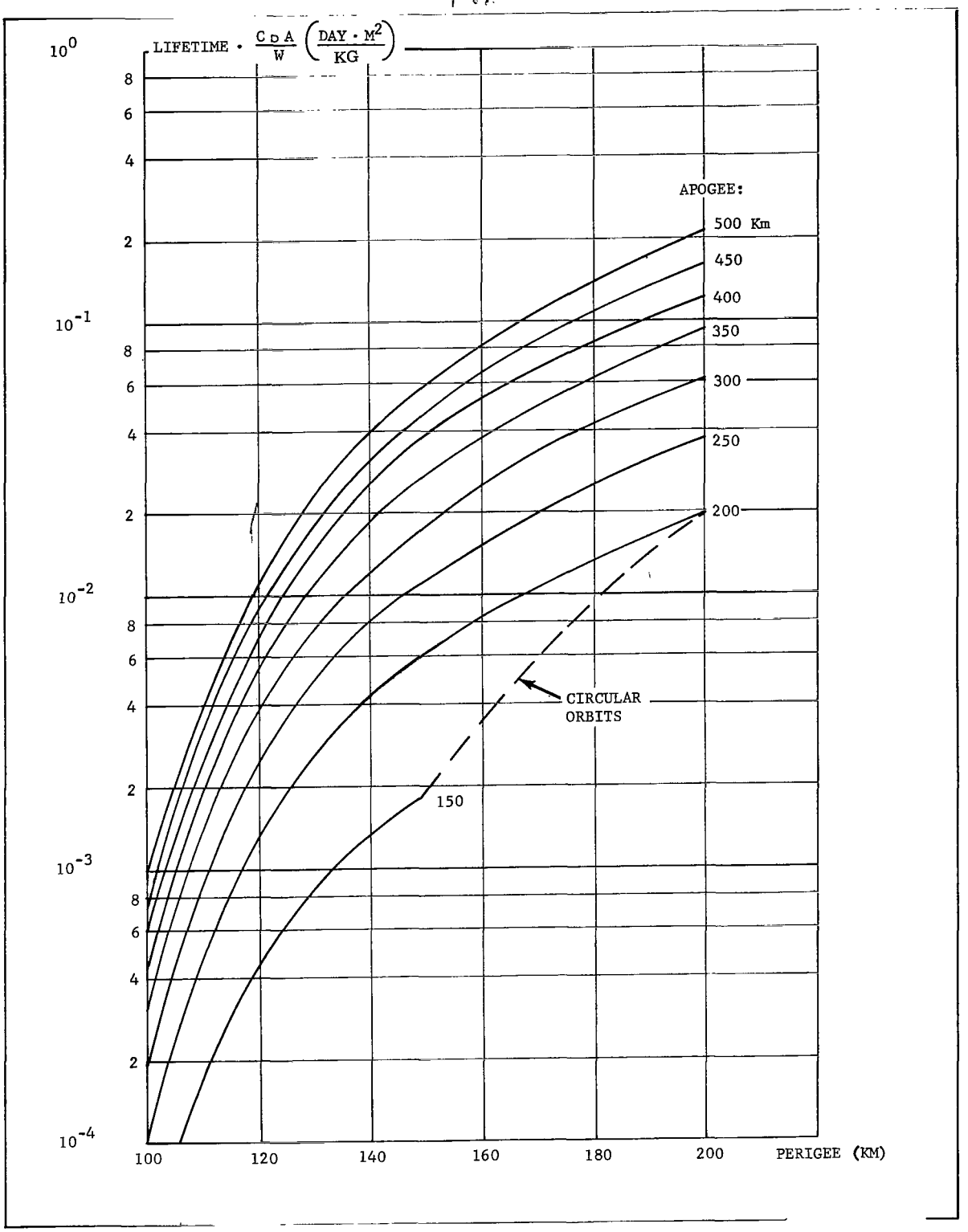

FIGURE 12. ORBITAL LIFETIME: 100-200 KM ALTITUDE REGION

REFERENCES

1. Sterne, Theodore E., "An Atmospheric Model, and Some Remarks on the Inference of Density From the Orbit of a Close Earth Satellite," Astronomical Journal 63, No. 3, March, 1958.

2. Kurtz, F. and McNair, A., "Satellite Lifetime," ABMA Report No. DA-TN-9-59, January 29, 1959.

3. Minzner, R. A., Champion, K. S. W., and Pond, H. L., "The ARDC Model Atmosphere," 1959, Air Force Survey in Geophysics No. 115, August 1959.

4. Wasko, P. E. and King, T. A., "Earth's Aerospace Properties from 100-100,000 km Altitude," MTP-AERO-63-2, January 3, 1963.

5. Priester, W., Martin, H. A., and Kamp, K., "Earth Satellite Observation and the Upper Atmosphere," "Nature", Vol. 188, Oct. 15, 1960.

6. Jacchia, L. G., "Solar-Effects on the Acceleration of Artificial Satellites," Smithsonian Special Report No. 29, Sept. 21, 1959.

7. Jacchia, L. G., "A Variable Atmospheric - Density Model From Satellite Accelerations," Smithsonian Special Report No. 39, March 30, 1960.

8. Sanger, Eugene, "The Gas Kinetics of Very High Flight Speeds," NACA Tech Memo 1270, 1950.

9. Martin, W. A., "A Review of the Forces and Heat Transfer Characteristics of Bodies in Free-Molecule Flow," Convair Report ERR-SD-003, 1960.

10. Stalder, Jackson R., et al, "A Comparison of Theory and Experiment for High-Speed Free-Molecule Flow," NACA Report 1032, 1951.

11. Stalder, Jackson R. and Zurick, Vernon J., "Theoretical Aerodynamic Characteristics of Bodies in a Free-Molecule-Flow Field," NACA Tech Note 2423, 1951.

12. Schamberg, R., "A New Analytic Representation of Surface Interaction for Hyperthermal Free Molecule Flow With Application to Neutral-Particle Drag Estimates of Satellites," ASTIA Doc. No. AD215301, 1959.

13. Payne, R. G., "Free Molecule Drag Coefficients of Convex Body Shapes." Available from Aeroballistics Division, George C. Marshall Space Flight Center, Huntsville, Alabama.

REFERENCES (Concluded)

14. Hartnett, J. P., "A Survey of Thermal Accommodation Coefficients," Advances in Applied Mechanics, Supplement 1, pp. 1-26, Academic Press, 1960.

15. Nocilla, Silvio, "On The Interaction Between Stream and Body in Free-Molecule Flow," Advances in Applied Mechanics, Supplement 1, pp. 169-207, Academic Press, 1960.

16. Jensen, J., Townsend, G., Kraft, J., and Kork, D., "Design Guide To Orbital Flight," McGraw-Hill Book Company, Inc., New York 1962.